Electronic Supplementary Material (ESI) for Journal of Materials Chemistry A.

Promoting Electrocatalytic Activity of Cobalt Cyclotetraphosphate in Full Water Splitting by Titanium-Oxide-Accelerated Surface Reconstruction

Cuncai Lv,[a,b,d] Shichen Xu,[a,d] Qianpeng Yang,[c] Zhipeng Huang*[a] and Chi Zhang*[a]

[a] School of Chemical Science and Engineering, Tongji University, Shanghai, PR China.

[b] Hebei Key Lab of Optic-electronic Information and Materials, The College of Physics Science and Technology, Hebei University, Baoding, PR China.

[c] School of Materials Science and Engineering, Jiangsu University, Zhenjiang, PR China.

[d] These authors made equal contribution to this work.

*Corresponding author. Zhipeng Huang (zphuang@tongji.edu.cn)

Chi Zhang (chizhang@tongji.edu.cn)

Electronic Supplementary Information

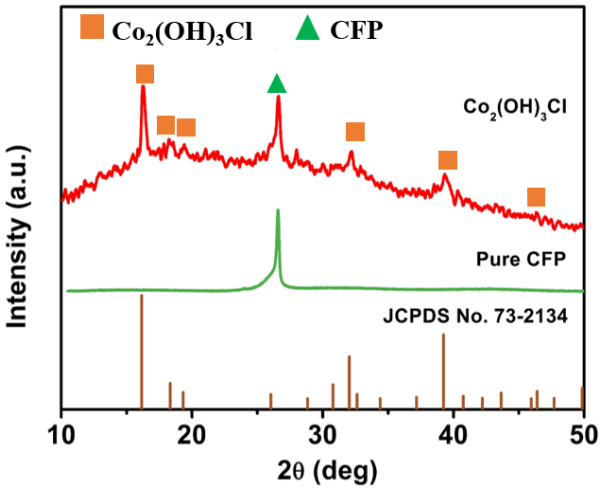

Figure S1. XRD pattern of $Co_2(OH)_3Cl$ prepared by thermal annealing the precursor ink on CFP.

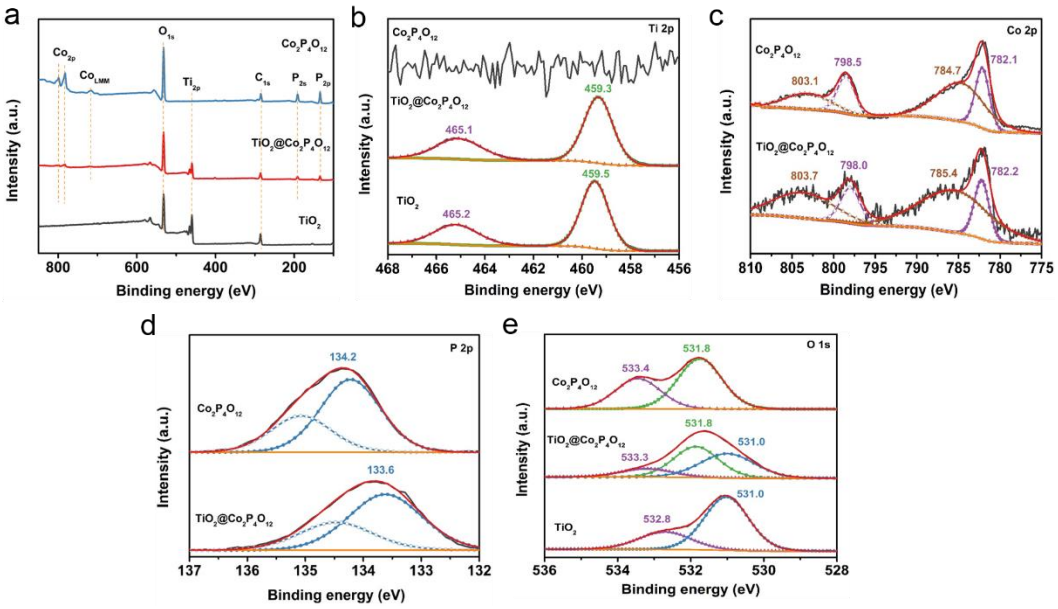

Figure S2. (a) Survey spectrum, (b) Ti 2p, (c) Co 2p, (d) P 2p and (e) O 1s high-resolution XPS spectra of $Co_2P_4O_{12}$, $TiO_2@Co_2P_4O_{12}$ and TiO_2.

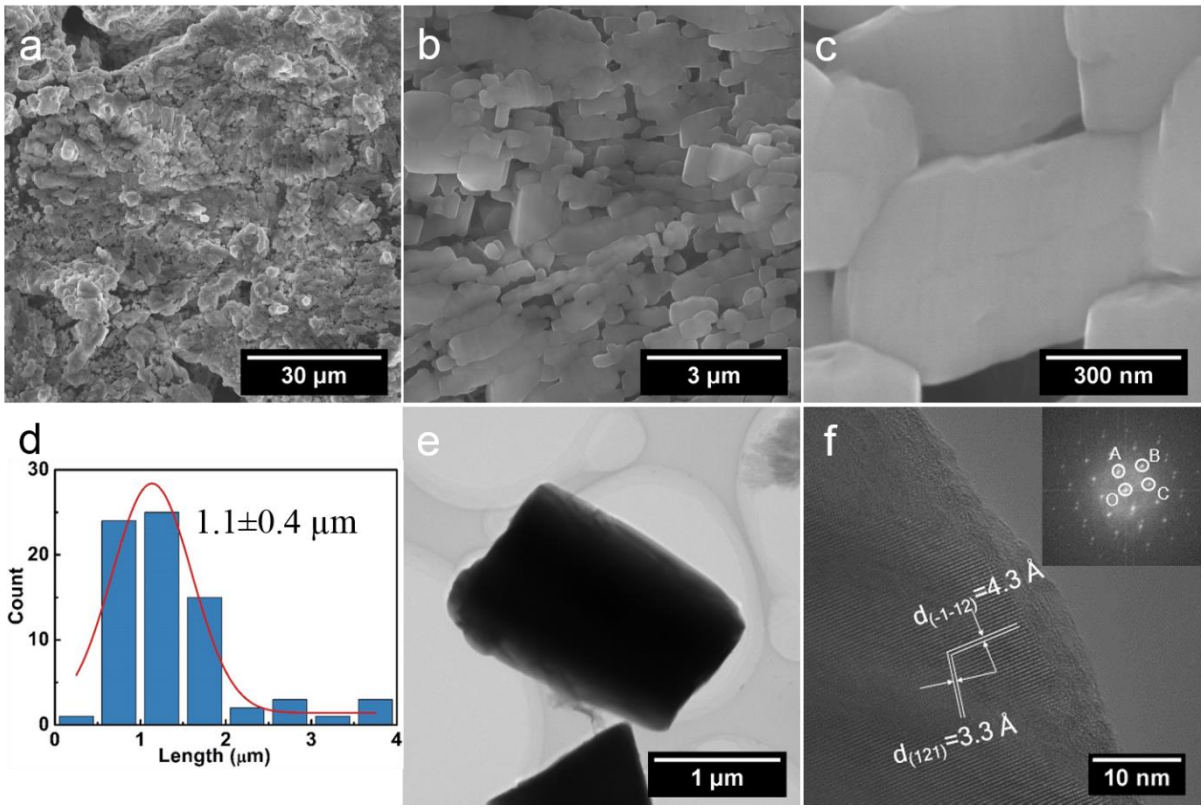

Figure S3. (a-c) SEM images of $Co_2P_4O_{12}$. (d) The size distribution of the $Co_2P_4O_{12}$ particles. (e) TEM and (f) HRTEM images of $Co_2P_4O_{12}$. Inset of (f) is the fast Fourier transform (FFT) pattern of lattice fringes in (f), which matches well with that of the [5 -3 1] zone axis diffraction pattern of monoclinic phase $Co_2P_4O_{12}$. ($1/d_{OA} = d_{(-1\ -1\ 2)}$ =4.3 Å, $1/d_{OB} = d_{(0\ 1\ 3)}$ =2.7 Å, $1/d_{OC} = d_{(1\ 2\ 1)}$ =3.3 Å, ∠AOB=55°, ∠BOC=40°).

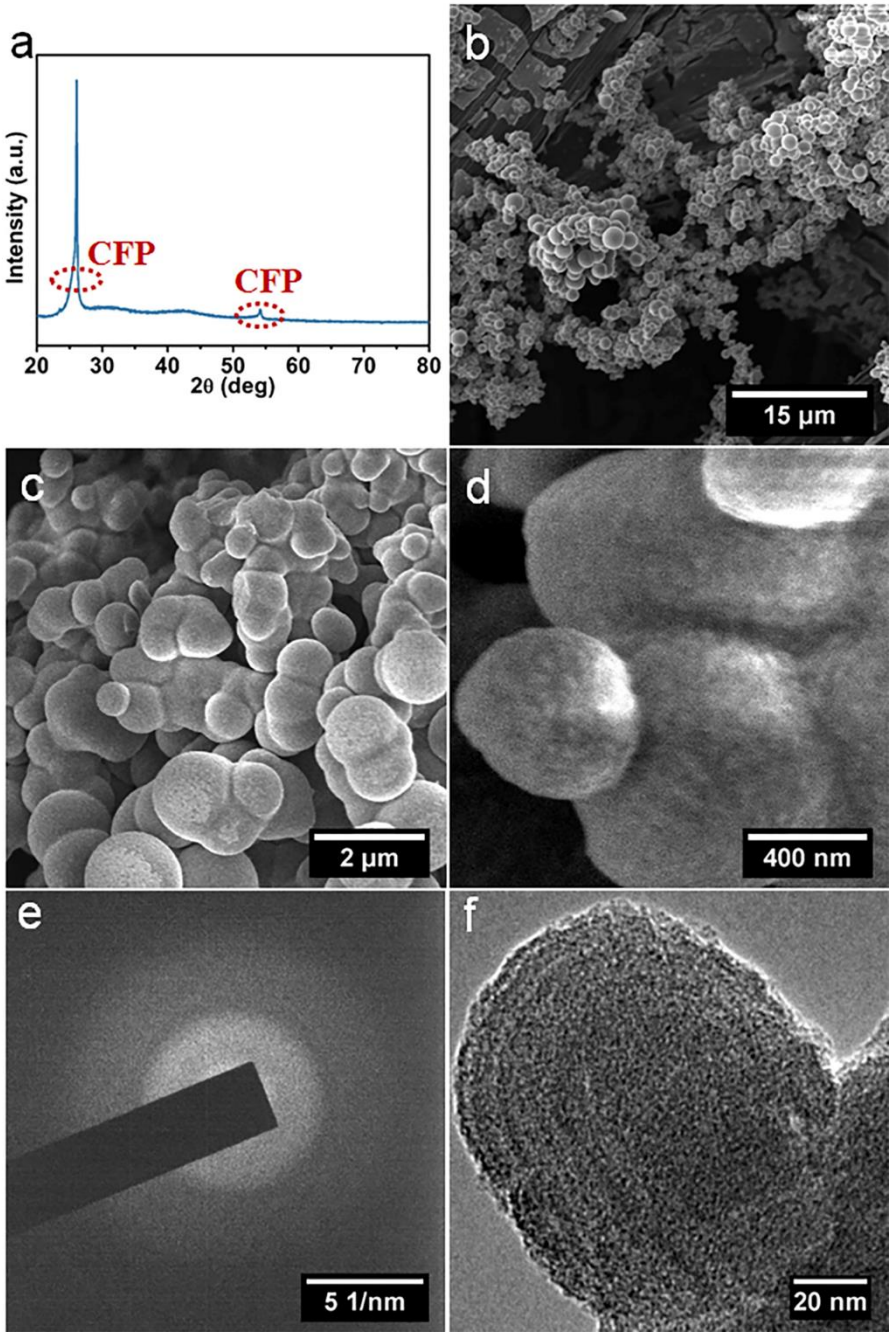

Figure S4. (a) XRD pattern of TiO_2 particles on CFP. (b, c) low- and (d) high- magnification SEM images of TiO_2. (e) TEM image and (f) SAED of TiO_2.

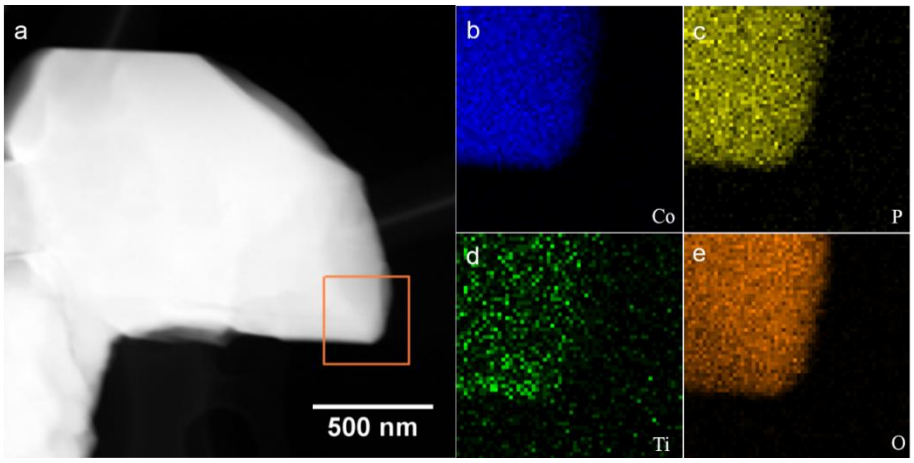

Figure S5. (a) STEM image and EDX elemental mapping images of (b) Co, (c) P, (d) Ti, and (e) O elements.

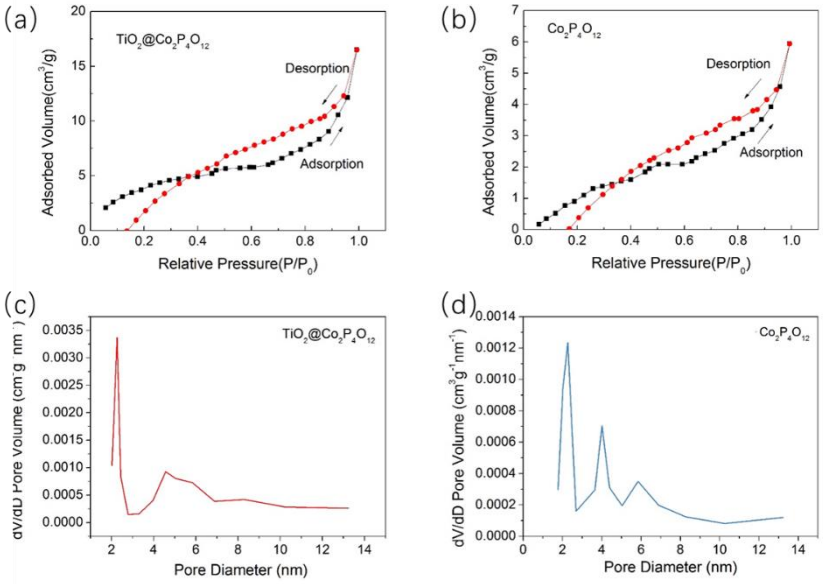

Figure S6. (a) N_2 adsorption–desorption isotherms and BJH pore-size distribution plots of the samples: (a,c) $TiO_2@Co_2P_4O_{12}$, and (b,d) $Co_2P_4O_{12}$.

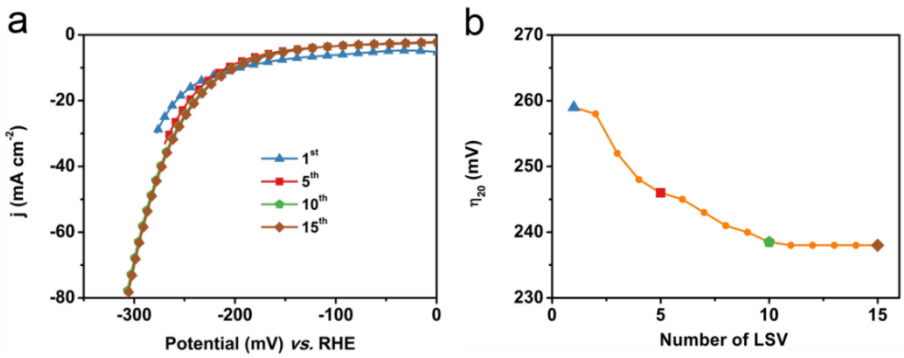

Figure S7. (a) Polarization curves corresponding to different LSV activation of $Co_2P_4O_{12}$. (b) Plot of η_{20} *versus* LSV scan number of $Co_2P_4O_{12}$.

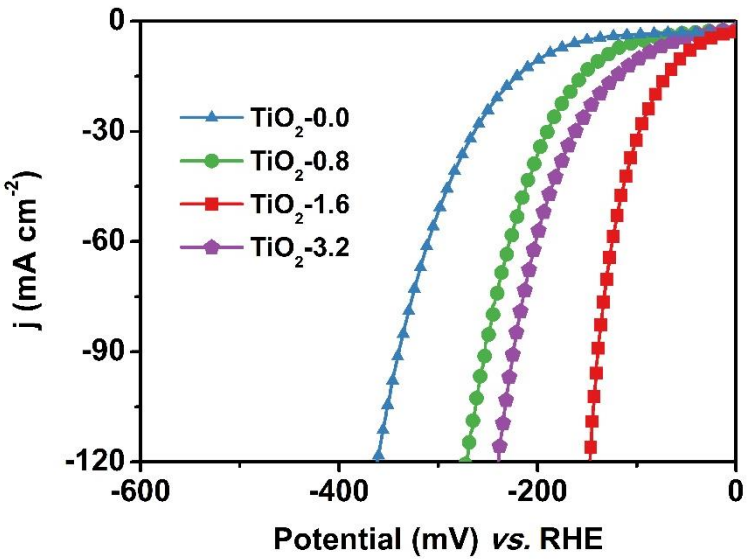

Figure S8. Polarization curves of TiO_2@$Co_2P_4O_{12}$(A) samples corresponding to different amount of TiO_2. Samples were referenced as TiO_2-X (X=0.0, 0.8, 1.6, 3.2), where X is the concentration (mM) of tetrabutyl titanate in the precursor solution.

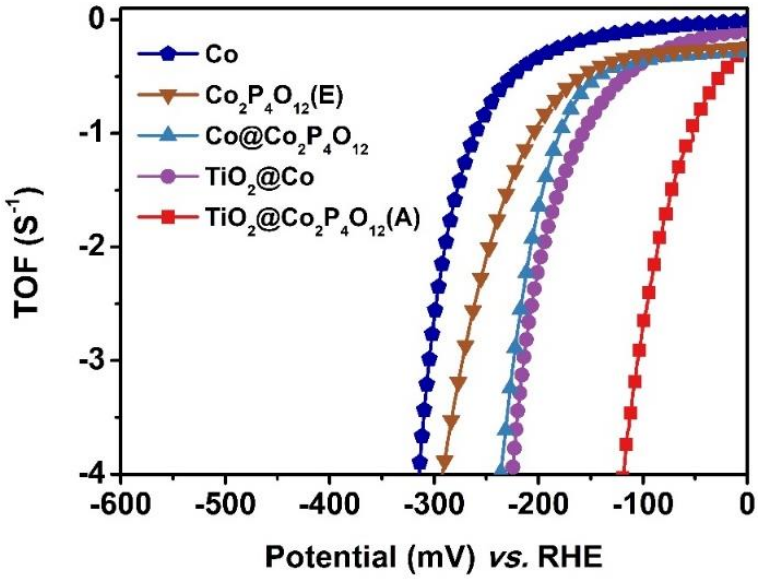

Figure S9. TOF plots of $TiO_2@Co_2P_4O_{12}$(A) and comparative samples in the HER.

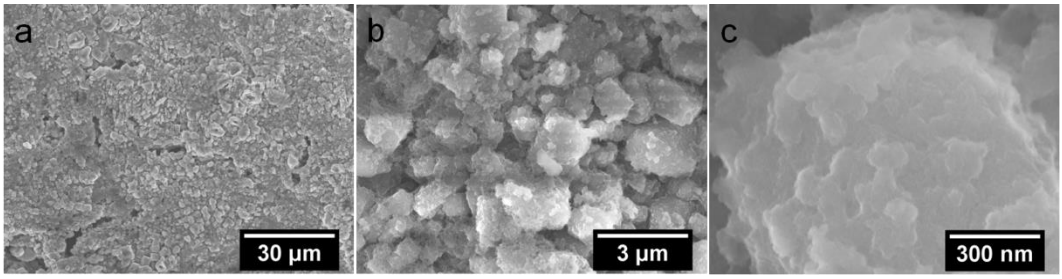

Figure S10. SEM images of TiO_2@$Co_2P_4O_{12}$(A) after a potentiostatic electrolysis for 40 h.

Table S1. Performance of typical metal phosphide/phosphate catalysts reported HER electrocatalysts in alkaline media.

Reference	Catalyst	Mass density (mg cm^{-2})	η_{20} (mV)	η_{100} (mV)	Tafel slope (mV/dec)	J_0 (mA cm^{-2})	Counter electrode	Electrolyte
This work	TiO_2@$Co_2P_4O_{12}$(A)	13	81	142	87	2.307	Graphite rod	1 M KOH
Applied Catalysis B: Environmental 204 (2017) 486–496	$Ni_{12}P_5$/$Ni_3(PO_4)_2$-HS	0.71	140	--	93.1		Platinum Pt	1 M KOH
Angew. Chem. Int. Ed. 2015, 54, 1 – 6	Ni_5P_4/ Ni foil	--	170	--	53	-- --	Coiled platinum wire	1 M KOH
Adv. Funct. Mater. 2016, 26, 4067–4077	CP@Ni-P	25.8	150	250	85.4	--	Graphite plate	1 M KOH
Angew. Chem. 2016, 128, 1 – 6	Ni_2P/NF	0.8	140	250	--	--	Pt wire	1 M KOH
Nano Energy 30 (2016) 303–311	Co_2P/CNT	0.75	160	325	103	--	Pt wire	1 M KOH
ACS Nano 2016, 10, 8738−8745	CoFePO (Fe O-doped Co_2P Ni foam)	2.187	120	290	38.1	--	Graphite rod	1 M KOH
Adv. Mater. 2015, 27, 3175–3180	Co phosphide/phosphate	0.1	410	--	--	--	Platinum foil	1 M KOH
Adv. Mater. 2018, 30, 1703322	CoO_x/CoP	--	70	146	42.8	--	Graphite bar	1 M KOH
Nanoscale, 2017, 9, 4793–4800	Al-CoP/CC	5.7	48	80	45	--	Graphite rod	1 M KOH
Angew. Chem. 2015, 127, 6349 –6352	Co-P films	2.71	104	150	42	--	--	1 M KOH
Nano Lett. 2016, 16, 7718−7725	NiCoP/NF	1.6	45	--	37	1.36	Graphite rod	1 M KOH
Energy Environ. Sci., 2015, 8, 2347	Ni_2P on Ni foam	1.8	255	--	--	--	Platinum wire	1 M KOH

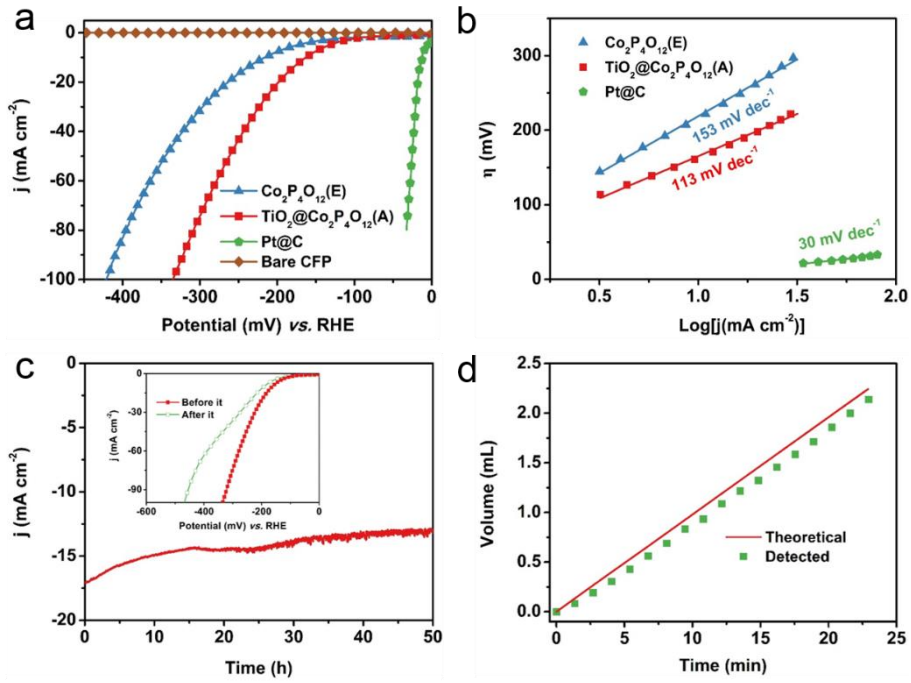

Figure S11. (a) Polarization curves and (b) corresponding Tafel plots for TiO_2@$Co_2P_4O_{12}$(A) in 0.5 M H_2SO_4 for HER. All potentials were corrected with iR drop. (c) Chronoamperometric curve of TiO_2@$Co_2P_4O_{12}$(A) measured at η = 200 mV *versus* RHE in 0.5 M H_2SO_4. Inset of Figure S9c is polarization curves of TiO_2@$Co_2P_4O_{12}$(A) measured before and after potentiostatic electrolysis experiments. (d) Current efficiency for H_2 produce under potentiostatic electrolysis experiment.

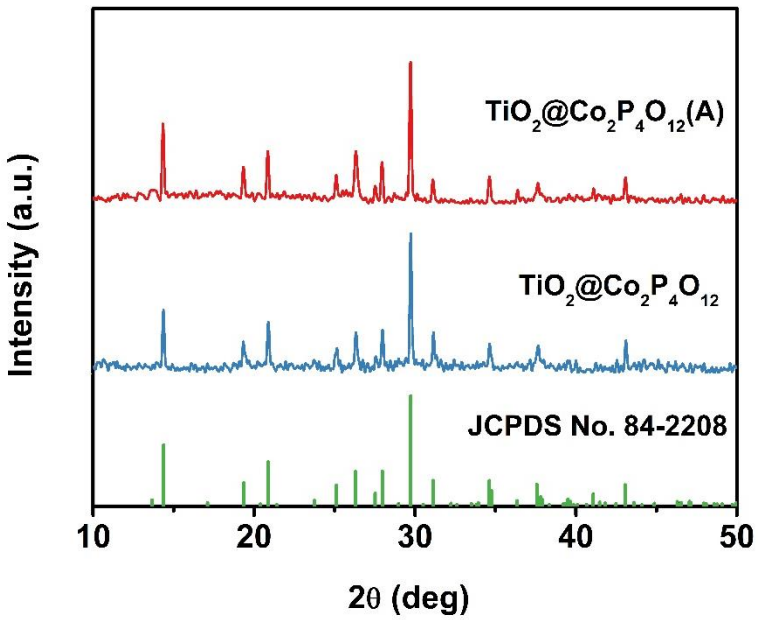

Figure S12. XRD pattern of $TiO_2@Co_2P_4O_{12}$(A) and $TiO_2@Co_2P_4O_{12}$.

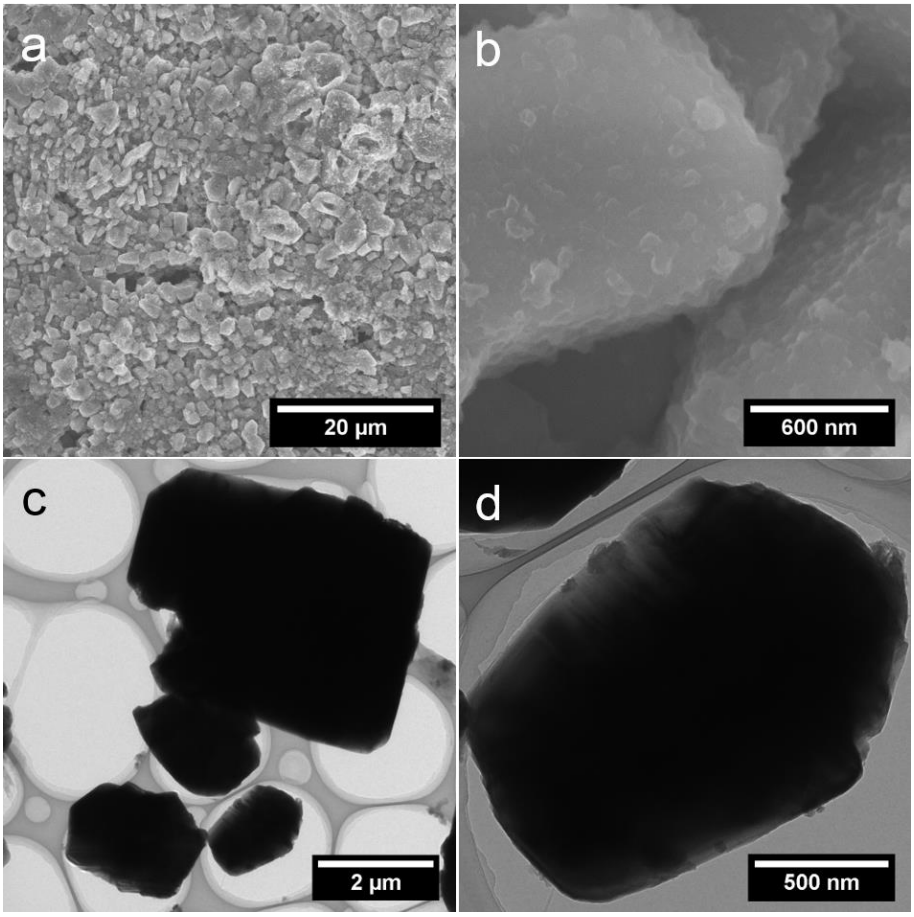

Figure S13. (a, b) SEM and (c, d) TEM images of TiO_2@$Co_2P_4O_{12}$(A).

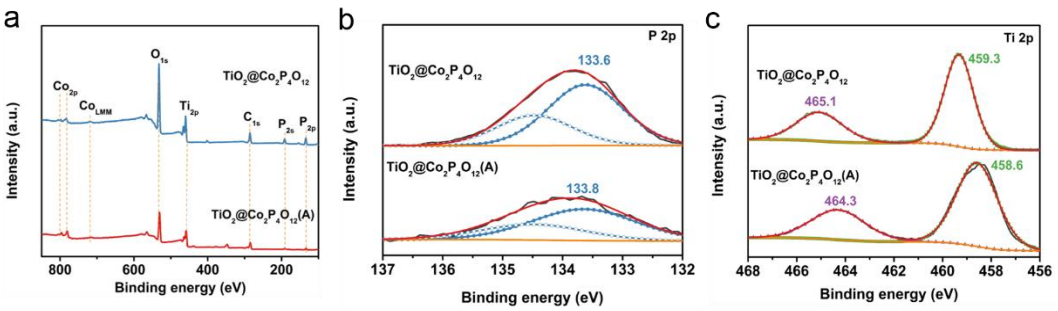

Figure S14. (a) XPS survey spectra, (b) P 2p (c) Ti 2p high-resolution XPS spectra of $TiO_2@Co_2P_4O_{12}$ and $TiO_2@Co_2P_4O_{12}$(A).

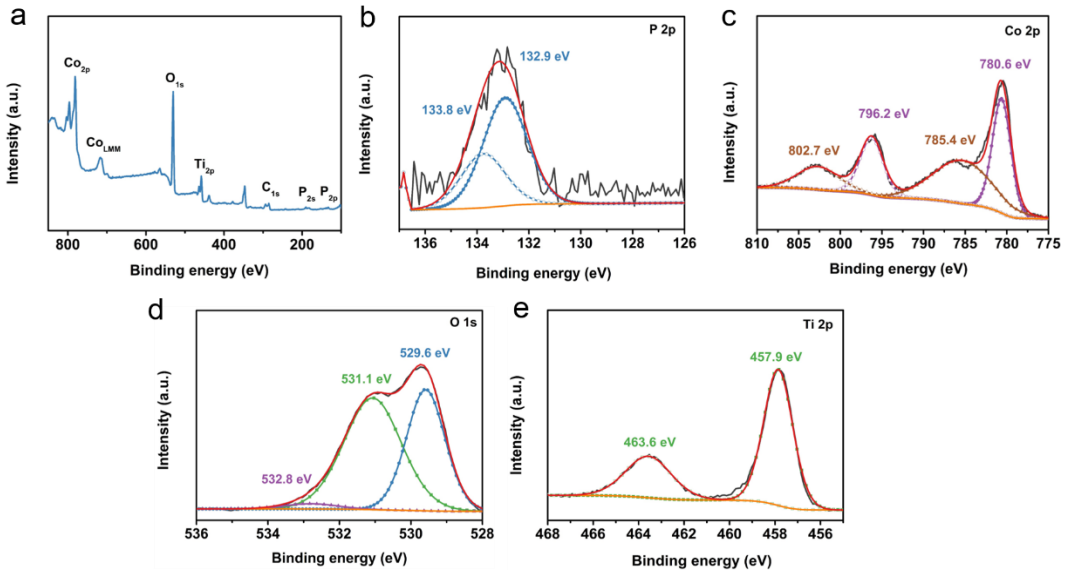

Figure S15. (a) XPS survey spectra, (b) P 2p, (c) Co 2p, (d) O 1s and (e) Ti 2p high-resolution XPS spectra of TiO_2@$Co_2P_4O_{12}$(jt).

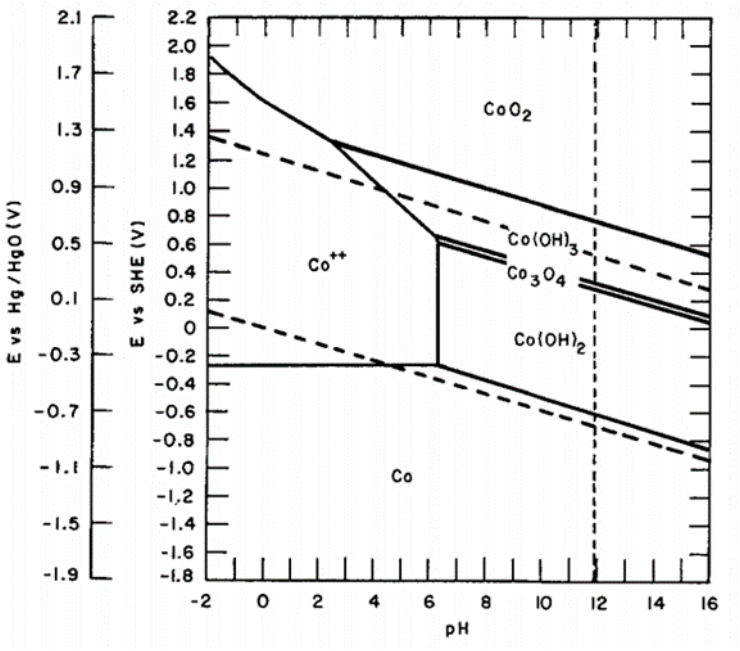

Figure S16. The Pourbaix diagram of cobalt.[1]

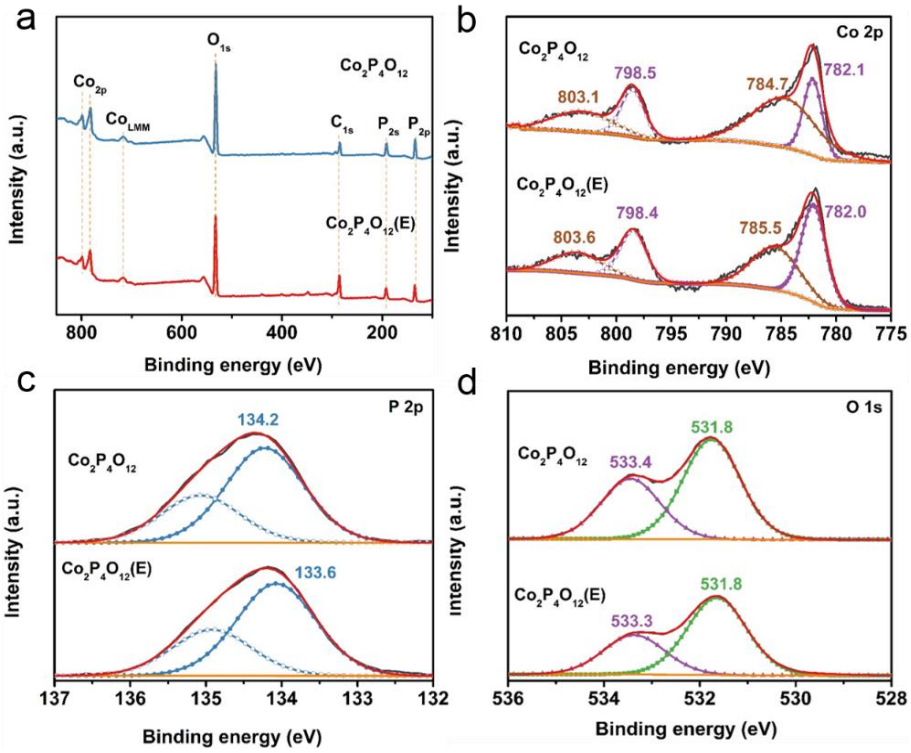

Figure S17. (a) XPS survey spectra, (b) Co 2p, (c) O 1s, and (d) O 1s high-resolution XPS spectra of $Co_2P_4O_{12}$ and $Co_2P_4O_{12}$(E).

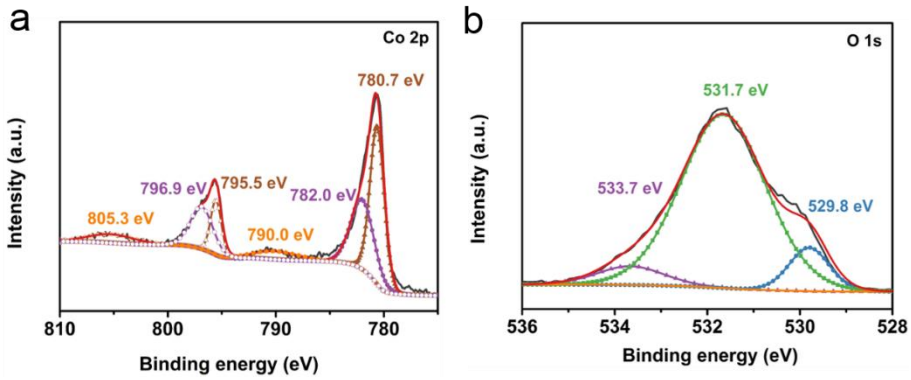

Figure S18. (a) Co 2p, (b) O 1s high-resolution XPS spectra of $Co_2P_4O_{12}$(jt).

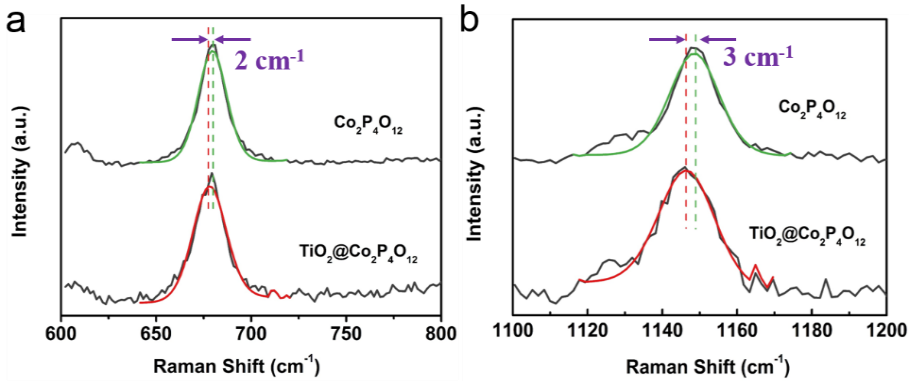

Figure S19. Raman spectra of $Co_2P_4O_{12}$ and $TiO_2@Co_2P_4O_{12}$.

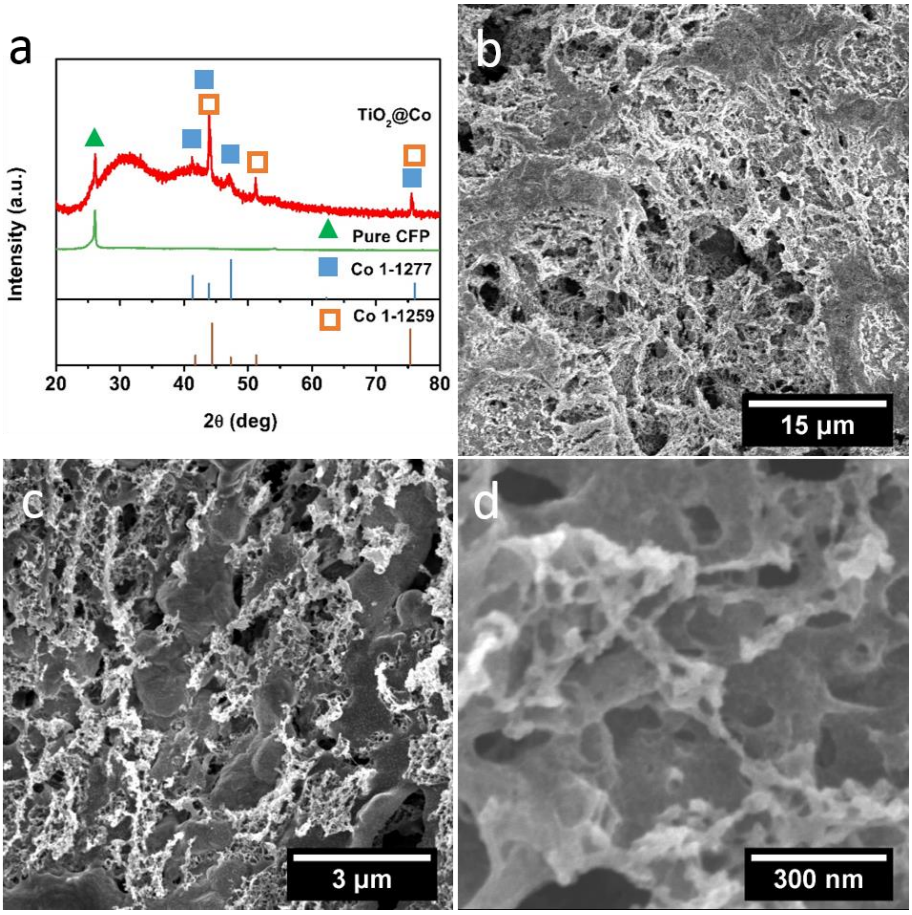

Figure S20. XRD pattern of TiO_2@Co. (b, c, d) SEM images of TiO_2@Co.

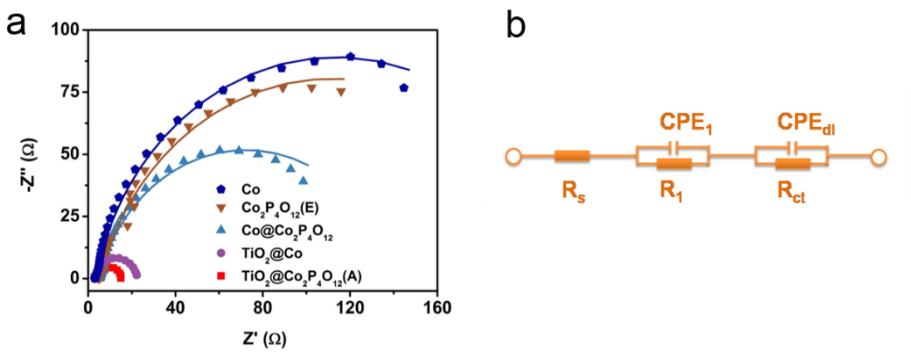

Figure S21. (a) EIS spectra of Co, $Co_2P_4O_{12}$(E), Co@$Co_2P_4O_{12}$, TiO_2@Co and TiO_2@$Co_2P_4O_{12}$(A) in the HER measured in 1 M KOH at η=100 mV. (b) Equivalent circuit used for fitting of EIS data. R_s is the overall series resistance, CPE_1 and R_1 are the constant phase element and resistance describing electron transport at substrate/catalyst interface, respectively, CPE_{dl} is the constant phase element of the catalyst/electrolyte interface, and R_{ct} is the charge transfer resistance at catalyst/electrolyte interface.

Table S2. The fitting results of EIS spectra in 1 M KOH for the HER.

Sample	R_s (Ω)	Q_1 (F S^{n-1})	n_1	R_1 (Ω)	Q_{dl} (F S^{n-1})	N_{dl}	R_{ct} (Ω)
Co	6.697E-4	0.00162	0.8663	3.475	0.03411	0.0.2094	220.2
$Co_2P_4O_{12}$(E)	2.042	6.961E-7	0.9674	3.043	0.04185	0.8181	213.0
Co@$Co_2P_4O_{12}$	2.131	1.054E-6	0.9351	2.992	0.04253	0.8369	134.1
TiO_2@Co	0.5596	1.111E-5	0.9054	2.746	0.05511	0.859	19.1
TiO_2@$Co_2P_4O_{12}$(A)	1.386	2.004E-6	0.9251	2.987	0.04011	0.8369	11.1

Table S3. The fitting results of free energies corresponding to different steps during the HER.

Sample	ΔG_{-V}^{*0} (meV)	ΔG_{+H}^{*0} (meV)	ΔG_{+T}^{*0} (meV)	ΔG_{ad}^{0} (meV)	R^2 (%)	$\Delta G_{+H}^{*0} - \Delta G_{ad}^{0}$ (meV)
$Co_2P_4O_{12}$(E)	359	548	1282	105	96.5	443
Co	241	603	1385	200	98.4	403
Co@$Co_2P_4O_{12}$	200	578	1250	182	99.97	396
TiO_2@Co	165	452	1078	80	98.98	372
TiO_2@$Co_2P_4O_{12}$(A)	105	420	1057	99	99.44	321

ΔG_{-V}^{*0}: the standard activation free energy for Volmer step.
ΔG_{+H}^{*0}: the standard activation free energy for Heyrovsky step.
ΔG_{+T}^{*0}: the standard activation free energy for Tafel step.
ΔG_{ad}^{0}: the standard free energy of adsorption for the reaction intermediate.
R^2 : goodness of data fitting.

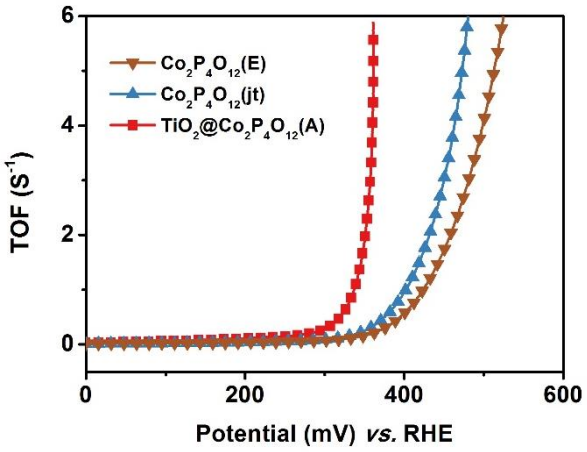

Figure S22. TOF plots of TiO_2@$Co_2P_4O_{12}$(A) and comparative samples in the OER.

Table S4. Performance of typical reported OER electrocatalysts in alkaline media.

Reference	Catalyst	Mass density (mg cm^{-2})	η_{20} (Potential, V)	η_{100} (Potential, V)	Tafel slope (mV/dec)	Counter electrode	Electrolyte
This work	TiO_2@$Co_2P_4O_{12}$	13	330	361	44.0	Graphite rod	1 M KOH
Applied Catalysis B: Environmental 204 (2017) 486–496	$Ni_{12}P_5/Ni_3(PO_4)_2$-HS	0.71	330	--	51.7	Platinum Pt	1 M KOH
Angew. Chem. Int. Ed. 2015, 54, 1 – 6	Ni_5P_4/ Ni foil	--	170	--	--	Coiled platinum wire	1 M KOH
Adv. Funct. Mater. 2016, 26, 4067–4077	CP@Ni-P	25.8	180	--	73	Graphite plate	1 M KOH
Angew. Chem. 2016, 128, 1 – 6	Ni_2P/NF	0.8	370	--	--	Pt wire	1 M KOH
Nano Energy 30 (2016) 303–311	Co_2P/CNT	0.75	345	495	103	Pt wire	1 M KOH
ACS Nano 2016, 10, 8738−8745	CoFePO	2.187	290	420	51.7	Graphite rod	1 M KOH
Adv. Mater. 2015, 27, 3175–3180	PCPTF	0.1	320	--	65	Platinum foil	1 M KOH
ACS Sustainable Chem. Eng. 2017, 5, 571−579	CC/NPC/CP	--	380	580	--	Pt wire	0.1 M KOH
Pans, 2017, 114, 5607-5611	$Fe(PO_3)_2/Ni_2P$	8	--	221	51.9	Pt wire	1 M KOH
Angew. Chem. 2015, 127, 6349 –6352	Co-P films	2.71	440	514	69	--	1 M KOH
Angew. Chem. 2015, 127, 9483 –9487	NiSe/NF	2.8	270	314	64	Graphite plate	1 M KOH
Angew. Chem. Int. Ed. 2016, 55, 6290 –6294	$NiCo_2O_4$ hollow microcuboids	1	298	345	53	Graphite rod	1 M NaOH
Nano Lett. 2016, 16, 7718−7725	NiCoP/NF	1.6	310	--	87	Graphite rod	1 M KOH
Energy Environ. Sci., 2015, 8, 2347	Ni_2P	0.14	305	--	59	Platinum wire	1 M KOH
Adv. Energy Mater. 2016, 6, 1502313	Co_2B-500 Co_2B-500/NG	0.21	410 370	-- --	-- --	Platinum cylindrical mesh	0.1 M KOH

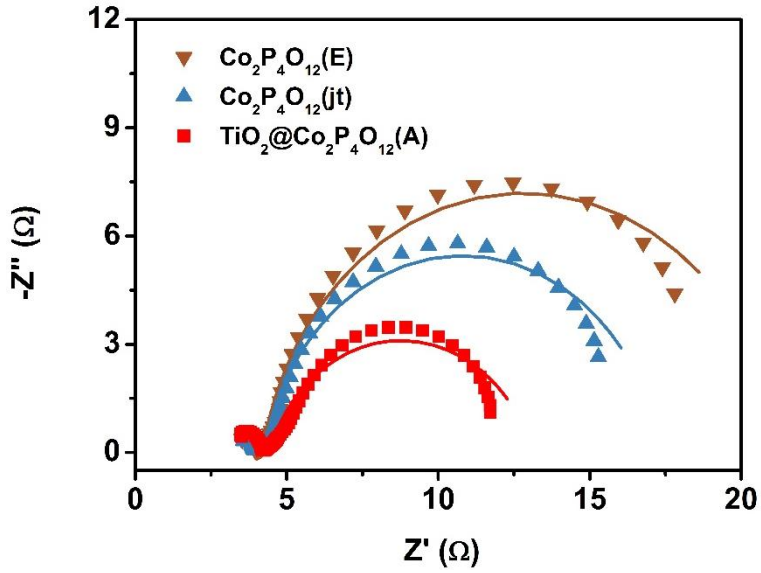

Figure S23. EIS spectra of TiO_2@$Co_2P_4O_{12}$(A), $Co_2P_4O_{12}$(E), and $Co_2P_4O_{12}$(jt) in the OER. The spectra were measured at η=350 mV.

Table S5. The fitting results of EIS spectra in 1 M KOH for the OER.

Sample	R_s (Ω)	Q_1 ($F\ S^{n-1}$)	n_1	R_1 (Ω)	Q_{dl} ($F\ S^{n-1}$)	N_{dl}	R_{ct} (Ω)
$Co_2P_4O_{12}$(E)	1.548E-4	4.943E-4	0.3138	4.217	0.2536	0.8861	27.11
Co@$Co_2P_4O_{12}$	4.298E-4	1.943E-4	0.2182	4.306	0.2332	0.8861	13.04
TiO_2@$Co_2P_4O_{12}$(A)	2.746E-5	1.054E-4	0.4407	4.413	0.2161	0.7871	8.715

Table S6. Performance of typical reported overall water splitting electrocatalysts in alkaline media.

Reference	Catalyst	Mass density (mg cm^{-2})	P_{20} (Potential, V)	P_{100} (Potential, V)	Counter electrode	Electrolyte
This work	TiO_2@$Co_2P_4O_{12}$	13	1.664	1.769	Graphite rod	1 M KOH
Applied Catalysis B: Environmental 204 (2017) 486–496	$Ni_{12}P_5$/$Ni_3(PO_4)_2$-HS	0.71	--	1.57	Platinum Pt	1 M KOH
Angew. Chem. Int. Ed. 2015, 54, 1 – 6	Ni_5P_4/ Ni foil	--	1.4	--	Coiled platinum wire	1 M KOH
Adv. Funct. Mater. 2016, 26, 4067–4077	CP@Ni-P	25.8	1.7	2.6	Graphite plate	1 M KOH
Nano Energy 30 (2016) 303–311	Co_2P/CNT	0.75	1.625	--	Pt wire	1 M KOH
ACS Nano 2016, 10, 8738−8745	CoFePO	2.187	1.64	1.96	Graphite rod	1 M KOH
Adv. Mater. 2015, 27, 3175–3180	PCPTF	0.1	1.57	--	Platinum foil	1 M KOH
Chem. Commun., 2015, 51, 16683--16686	CoSe/Ti	3.8	1.69	1.9	Graphite plate	1 M KOH
Angew. 2015, 127, 9483 –9487	NiSe/NF	2.8	1.75	--	Graphite plate	1 M KOH
Angew. Chem. Int. Ed. 2016, 55, 6290 –6294	$NiCo_2O_4$ hollow microcuboids	1	1.74	--	Graphite rod	1 M NaOH
Nano Lett. 2016, 16, 7718−7725	NiCoP/NF	1.6	1.625	1.82	Graphite rod	1 M KOH
Energy Environ. Sci., 2015, 8, 2347	Ni_2P on Ni foam	5	1.7	--	Platinum wire	1 M KOH
Adv. Energy Mater. 2016, 6, 1502313	Co_2B-500 &Co_2B-500/NG	0.21	1.95	--	Platinum cylindrical mesh	3 M KOH

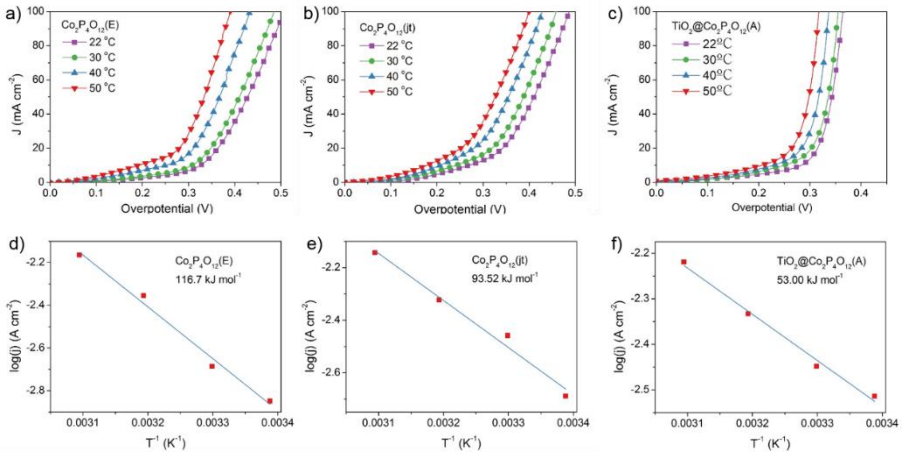

Figure S24. Polarization curves of (a) $Co_2P_4O_{12}$(E), (b) $Co_2P_4O_{12}$(jt), and (c) TiO_2@ $Co_2P_4O_{12}$(A). Arrhenius plots of (d) $Co_2P_4O_{12}$(E), (e) $Co_2P_4O_{12}$(jt), and (f) TiO_2@ $Co_2P_4O_{12}$(A) at the overpotential of 150 mV.

References

(1) M. Pourpaix, *Atlas of electrochemical equilibria in aqueous solutions*, National Association of Corrosion Engineers, Houston **1974**.